Modelling of Unsaturated Flow Through Porous Media Using Meshless Methods

Mohamed Boujoudar, Abdelaziz Beljadid, and Ahmed Taik

1 Introduction

The process of infiltration through porous media is an important part of hydrological cycle. The modelling of this process has important practical applications in engineering such as water resources management and agriculture. Most numerical models that describe the unsaturated flow in soils use the Richards model [16] which is a highly nonlinear equation. This equation is obtained from Darcy's law and the conservation of mass [2]. The strong non-linearity of the unsaturated conductivity and the capillary pressure as functions of saturation and the presence of both advection and diffusion terms make the Richards equation more challenging in terms of numerical approximations and require the development of efficient numerical techniques. The unsaturated conductivity and capillary pressure are correlated using empirical models and experiment data such as the van Genuchten [20], Brooks-Corey [4] and Gardner [6] models. Analytical solutions of the Richards equation can only obtained for some cases with special initial and boundary conditions [7, 17–19]. Therefore, different numerical techniques are developed to efficiently solve the Richards equation such as, finite-difference, finite-element, and finite-volume

M. Boujoudar (✉) · A. Beljadid
Mohammed VI Polytechnic University, Green City, Morocco
e-mail: mohamed.boujoudar@um6p.ma

A. Beljadid
e-mail: abdelaziz.beljadid@um6p.ma

A. Beljadid
University of Ottawa, Ottawa, Canada

A. Taik
FST-Mohammedia, University Hassan II, Casablanca, Morocco
e-mail: ahmed.taik@fstm.ac.ma

© Canadian Society for Civil Engineering 2022

S. Walbridge et al. (eds.), *Proceedings of the Canadian Society of Civil Engineering Annual Conference 2021*, Lecture Notes in Civil Engineering 250,
https://doi.org/10.1007/978-981-19-1065-4_47

methods. For instance, Celia et al. [5] used the mixed form of the Richards equation and proposed a general mass-conservative numerical scheme, and Bause and Knabner [1] developed an adaptive mixed hybrid finite element discretization for the Richards equation. Manzini and Ferraris [15] developed a mass conservative finite volume method using two-dimensional unstructured grids. Although many numerical techniques have been developed to numerically solve the Richards equation, there is still a strong need for more robust numerical techniques for modelling flows in unsaturated soils.

The aim of this work is to develop a new technique based on the localized radial basis function method and the Kirchhoff transformation in order to solve Richards equation in one and two-dimensional homogeneous medium. The proposed technique allows us to avoid mesh generation, which makes the numerical method less expensive in terms of computational cost. The use of localized meshless method has the advantage of flexibility in dealing with complex geometries [3]. The proposed method performs well in terms of accuracy and efficiency for modelling unsaturated flow through soils.

To handle the nonlinearity of the Richards equation, we use the Kirchhoff transformation which allows us to reduce the nonlinearity of the studied problem. We used Picard iterations to solve the problem with the Kirchhoff variable where we used the backward Euler method for temporal discretization. Other numerical techniques using the Kirchhoff transformation to solve the Richards equation can be found in [8]. The performance of the proposed numerical method is assessed using different test cases.

The outline of the paper is as follows. In Sect. 2, we introduce the governing equation and the proposed system using the Kirchhoff transformation. In Sect. 3, we present the proposed meshless method. Numerical simulations are performed in Sect. 4 for modelling water flow through one and two-dimensional unsaturated porous media. Finally, we provide some conclusions in Sect. 5.

2 Governing Equation

2.1 The Mathematical Model

Infiltration of water in unsaturated soils is described by the Richards equation [16] which can be derived from Darcy's law and the conservation of mass. This equation is given by:

$$\frac{\partial \theta}{\partial t} + \nabla.(K \nabla h) + \frac{\partial K}{\partial z} = s(\boldsymbol{x}, t), \qquad \boldsymbol{x} \in \Omega, 0 \leq t \leq T, \tag{1}$$

where $\theta\left[\mathrm{L}^3/\mathrm{L}^3\right]$ is the moisture content, h[L] is the pressure head, K[L/T] is the unsaturated hydraulic conductivity, $\boldsymbol{x} = (x, y, z)^T$ is the coordinate vector, x[L]

and y[L] denote the horizontal dimensions and z[L] denotes the vertical dimension positive down (coordinate in the direction of gravity) and $s(\boldsymbol{x}, t)$ is a source or sink term which can depend on space and time and can include evaporation, plant root extraction, etc. In this study, we assume that $s(\boldsymbol{x}, t) = 0$, Ω is an open set of $\mathbb{R}^d (d = 1, 2, 3)$, and T is the final simulation time.

We note that the Richards equation can be expressed using the water saturation $S = \left(\frac{\theta - \theta_r}{\theta_s - \theta_r}\right)$ and the parameter $\phi = \theta_s - \theta_r$ where θ_s and θ_r are respectively the saturated and residual moisture contents. The unsaturated hydraulic conductivity is given by:

$$K = K_s k_r, \tag{2}$$

where k_r is the water relative permeability, which accounts for the effect of partial saturation and the saturated hydraulic conductivity is as follows:

$$K_s = \frac{\rho g k}{\mu}, \tag{3}$$

where ρ is the water density, g is the gravitational acceleration, k is the intrinsic permeability of the medium, and μ is the fluid dynamic viscosity. The Richards equation can be rewritten in the following form:

$$\phi \frac{\partial S}{\partial t} + \nabla.(K_s k_r \nabla h) + \frac{\partial (K_s k_r)}{\partial z} = 0, \quad \boldsymbol{x} \in \Omega, 0 \leq t \leq T, \tag{4}$$

Equation (4) is highly non-linear due to the nonlinearity of the hydraulic conductivity and the capillary pressure function. Constitutive relationships are available for the functions $S\left[\mathrm{L}^3/\mathrm{L}^3\right]$ and K[L/T] based on experiment. In our study, the numerical techniques will be developed based on Eq. (4) where we will introduce the Kirchhoff transformation in order to reduce the nonlinearity of the equation.

2.2 Capillary Pressure

The pressure head can be expressed as a function of saturation in the following form:

$$h(S) = h_{cap} J(S), \tag{5}$$

where $J(S)[-]$ is a dimensionless capillary pressure function and h_{cap}[L] is the capillary rise which is given by the classical Leverett scaling [13]:

$$h_{cap} \sim \frac{\gamma \cos \boldsymbol{\theta}}{pg\sqrt{\frac{k}{\phi_p}}}, \tag{6}$$

γ is the surface tension between the fluids, $\boldsymbol{\theta}$ is the contact angle and $\boldsymbol{\phi}$ is the medium porosity.

2.3 Kirchhoff Transformation

The Kirchhoff integral transformation is defined as:

$$\varphi(h) = \int_{+\infty}^{h} k_r(s)ds. \tag{7}$$

By applying this transformation, we can rewrite the Richards equation using the variable φ, as explained below:

$$\nabla.(K_s k_r \nabla h) = K_s \nabla^2 \varphi, \tag{8}$$

$$\frac{\partial \varphi}{\partial t} = k_r \frac{\partial h}{\partial t}, \quad \frac{\partial \varphi}{\partial z} = k_r \frac{\partial h}{\partial z}. \tag{9}$$

By transforming the derivative terms $\frac{\partial S}{\partial t}$ and $\frac{\partial}{\partial z}(K_s k_r)$ using the variable φ, we obtain:

$$\frac{\partial S}{\partial t} = \frac{\partial S}{\partial h}\frac{\partial h}{\partial t} = \left(k_r^{-1}\frac{\partial S}{\partial h}\right)\frac{\partial \varphi}{\partial t}, \tag{10}$$

$$\frac{\partial}{\partial z}(K_s k_r) = K_s \frac{\partial k_r}{\partial h}\frac{\partial h}{\partial z} = \left(K_s k_r^{-1}\frac{\partial k_r}{\partial h}\right)\frac{\partial \varphi}{\partial z}. \tag{11}$$

We consider the variables:

$$\begin{cases} A = \dfrac{\phi}{K_s}\left(k_r^{-1}\dfrac{\partial S}{\partial h}\right), \\ B = \left(k_r^{-1}\dfrac{\partial k_r}{\partial h}\right). \end{cases} \tag{12}$$

This leads to the following equation:

$$A\frac{\partial \varphi}{\partial t} + \nabla^2 \varphi + B\frac{\partial \varphi}{\partial z} = 0. \tag{13}$$

Finally, by applying the Kirchhoff transformation, we reduced the nonlinearity of Eq. (4) and obtain Eq. (13) which has many benefits in terms of convergence of the proposed numerical method.

2.4 Initial and Boundary Conditions

For the initial condition, we assume that the pressure head is $h(\boldsymbol{x}, 0) = h_0$ for each point $\boldsymbol{x}$ on the computational domain Ω, which can be expressed using the Kirchhoff variable as $\varphi(\boldsymbol{x}, 0) = \varphi(h_0)$.

We transform the boundary conditions using the Kirchhoff variable in a similar way:

Dirichlet: $h(\boldsymbol{x}, t) = h_D$ for each $\boldsymbol{x} \in \partial\Omega$ leads to $\varphi(\boldsymbol{x}, t) = \varphi(h_D)$.

Neumann: $n_i \frac{\partial h}{\partial \boldsymbol{x}_i} = h_N$ implies $n_i \frac{\partial \varphi}{\partial \boldsymbol{x}_i} = k_r h_N$, with h_D and h_N are given functions and n_i is the unit normal vector to the boundary.

3 The Materials and Proposed Techniques

In this section, we propose an efficient computational technique based on radial basis function collocation method [9, 10]. This method has recently become very popular due to its advantages in terms of approximation properties of solutions and its less computational cost since it does not require mesh generation.

Equation (13) is solved using the localized RBF collocation method and the Picard iteration technique. The temporal discretization of Eq. (13) using the backward Euler method is given by:

$$A^{n+1} \frac{\varphi^{n+1} - \varphi^n}{\Delta t} + \nabla^2 \varphi^{n+1} + B^{n+1} \frac{\partial \varphi^{n+1}}{\partial z} = 0, \tag{14}$$

where φ^{n+1}, A^{n+1} and B^{n+1} are the approximate values of φ, A and B at $t = t^{n+1}$, respectively. $\Delta t = t^{n+1} - t^n$ is the time setup and the solution is assumed to be known at t^n and unknown at t^{n+1}.

Equation (14) is linearized using the Picard iteration method which involves sequential estimation of the unknown φ^{n+1} using the latest estimates of A^{n+1} and B^{n+1}. If m identifies iteration levels, then the Picard iteration steps can be written as:

$$A^{m,n+1} \frac{\varphi^{m+1,n+1} - \varphi^n}{\Delta t} + \nabla^2 \varphi^{m+1,n+1} + B^{m,n+1} \frac{\partial \varphi^{m+1,n+1}}{\partial z} = 0. \tag{15}$$

For the sake of simplicity, we consider the following notations:

$$\mathcal{L}^m = \left(\frac{A^{m,n+1}}{\Delta t} . + \nabla^2 . + B^{m,n+1} \frac{\partial .}{\partial z} \right), \tag{16}$$

$$f^{m,n+1} = A^{m,n+1} \frac{\varphi^n}{\Delta t}, \tag{17}$$

$\mathcal{L}^m$ is a linear operator for each Picard iteration m. Subject to boundary and initial conditions, Eq. (15) can be rewritten in the following form:

$$\begin{cases} \mathcal{L}^m \varphi^{m+1,n+1}(\boldsymbol{x}) = f^{m,n+1}(\boldsymbol{x}), & \boldsymbol{x} \in \Omega, \\ \mathcal{B}\varphi^{m+1,n+1}(\boldsymbol{x}) = q(\boldsymbol{x}), & \boldsymbol{x} \in \partial\Omega, \\ \varphi^{m+1,0}(\boldsymbol{x}) = \varphi_0^{m+1}(\boldsymbol{x}), & \boldsymbol{x} \in \Omega, \end{cases} \tag{18}$$

$\mathcal{B}$ is a border operator, q is the given function associated with the boundary conditions. For each iteration n, Eq. (18) is solved using localized RBF meshless method at each Picard iteration m until the stop condition is verified which is given by:

$$\delta^m = \left| \varphi^{m+1,n+1} - \varphi^{m,n+1} \right| \leq Tol, \tag{19}$$

with Tol is the error tolerance.

3.1 Localized RBF Meshless Method

In this section, we present the local multiquadric (LMQ) method [11]. This approach is different from the traditional global multiquadric approximation since only local configuration of nodes are used. To recall the localized RBF techniques, let $\{\boldsymbol{x}_j\}_{j=1}^{n_i}$ and $\{\boldsymbol{x}_j\}_{j=n_i+1}^{N}$ be the collocation points in Ω and $\partial\Omega$, respectively. n_i is the number of interior points and N the total number of collocation points distributed over the computational domain. For each $\boldsymbol{x}_s \in \Omega$, we create a localized domain $\Omega^{[s]}$ that contains n_s nearest neighbors interpolation points $\left\{\boldsymbol{x}_k^{[s]}\right\}_{k=1}^{n_s}$ to $\boldsymbol{x}_s$.

In each localized domain $\Omega^{[s]}$, the approximate solution can be written as a linear combination of n_s multiquadric functions in the following form:

$$\varphi_{[s]}^{m+1,n+1}(\boldsymbol{x}_s) = \sum_{k=1}^{n_s} \alpha_k^{m+1,n+1} \Phi_k \left(\left\| \boldsymbol{x}_s - \boldsymbol{x}_k^{[s]} \right\| \right), \tag{20}$$

where $\left\{\alpha_k^{m+1,n+1}\right\}_{k=1}^{n_s}$ unknown coefficients to be determined, $||.||$ is the Euclidian norm and Φ_k are the multiquadric radial basis functions defined as:

$$\Phi_k(\boldsymbol{x}) = \Phi(r_k) = \sqrt{1 + (\varepsilon r_k)^2}, \tag{21}$$

where $\varepsilon > 0$ is the shape parameter and $r_k = \|\boldsymbol{x} - \boldsymbol{x}_k\|$. Equation (21) can be presented in the matrix form:

$$\varphi_{[s]}^{m+1,n+1} = \Phi^{[s]}\alpha_{[s]}^{m+1,n+1}, \tag{22}$$

where $\varphi_{[s]}^{m+1,n+1} = \left[\varphi_{[s]}^{m+1,n+1}\left(\boldsymbol{x}_1^{[s]}\right), \varphi_{[s]}^{m+1,n+1}\left(\boldsymbol{x}_2^{[s]}\right), \ldots, \varphi_{[s]}^{m+1,n+1}\left(\boldsymbol{x}_{n_s}^{[s]}\right)\right]^T$, $\alpha_{[s]}^{m+1,n+1} = \left[\alpha_{[s]}^{m+1,n+1}\left(\boldsymbol{x}_1^{[s]}\right), \alpha_{[s]}^{m+1,n+1}\left(\boldsymbol{x}_2^{[s]}\right), \ldots, \alpha_{[s]}^{m+1,n+1}\left(\boldsymbol{x}_{n_s}^{[s]}\right)\right]^T$ and $\Phi^{[s]}$ is an $n_s \times n_s$ real symmetric coefficient matrix defined as $\Phi^{[s]} = \left[\Phi\left(\left\|\boldsymbol{x}_i^{[s]} - \boldsymbol{x}_j^{[s]}\right\|\right)\right]_{1\le i,j\le n_s}$. The vector $\alpha_{[s]}^{m+1,n+1}$ can be obtained as the following equation:

$$\alpha_{[s]}^{m+1,n+1} = \left(\Phi^{[s]}\right)^{-1}\varphi_{[s]}^{m+1,n+1}. \tag{23}$$

For $\boldsymbol{x}_s \in \Omega$, we apply the differential operator $\mathcal{L}^m$ to Eq. (20) to obtain the following equation:

$$\mathcal{L}^m\varphi_{[s]}^{m+1,n+1}(\boldsymbol{x}_s) = \sum_{k=1}^{n_s}\alpha_k^{m+1,n+1}\mathcal{L}^m\Phi_k\left(\left\|\boldsymbol{x}_s - \boldsymbol{x}_k^{[s]}\right\|\right) = \sum_{k=1}^{n_s}\alpha_k^{m+1,n+1}\Psi^m\left(\left\|\boldsymbol{x}_s - \boldsymbol{x}_k^{[s]}\right\|\right),$$

$$\Theta_{[s]}^m\alpha_{[s]}^{m+1,n+1} = \Theta_{[s]}^m\left(\Phi^{[s]}\right)^{-1}\varphi_{[s]}^{m+1,n+1} = \Lambda_{[s]}^m\varphi_{[s]}^{m+1,n+1} = \Lambda^m\varphi^{m+1,n+1}, \tag{24}$$

where $\varphi^{m+1,n+1} = \left[\varphi^{m+1,n+1}(\boldsymbol{x}_1), \varphi^{m+1,n+1}(\boldsymbol{x}_2), \ldots, \varphi^{m+1,n+1}(\boldsymbol{x}_N)\right]^T$, $\Theta_{[s]}^m = \left[\Psi^m\left(\left\|\boldsymbol{x}_s - \boldsymbol{x}_1^{[s]}\right\|\right), \Psi^m\left(\left\|\boldsymbol{x}_s - \boldsymbol{x}_2^{[s]}\right\|\right), \ldots, \Psi^m\left(\left\|\boldsymbol{x}_s - \boldsymbol{x}_{n_s}^{[s]}\right\|\right)\right]^T$, $\Psi^m = \mathcal{L}^{\mathrm{m}}\Phi_{\mathrm{k}}$ and $\Lambda_{[s]}^m = \Theta_{[s]}^m\left(\Phi^{[s]}\right)^{-1}$.

In order to extend Eq. (24) to be able to use $\varphi^{m+1,n+1}$ instead of $\varphi_{[s]}^{m+1,n+1}$, we consider Λ^m as the expansion of $\Lambda_{[s]}^m$ which can be obtained by padding the local vector with zeros.

Similarly, for $\boldsymbol{x}_s \in \partial\Omega$, we create an influence domain $\Omega^{[s]}$ containing $\boldsymbol{x}_s$. Then we have:

$$\begin{aligned}\mathcal{B}\varphi^{m+1,n+1}(\boldsymbol{x}_s) &= \sum_{k=1}^{n_s}\alpha_k^{m+1,n+1}\mathcal{B}\Phi_k\left(\left\|\boldsymbol{x}_s - \boldsymbol{x}_k^{[s]}\right\|\right) = \left(\mathcal{B}\Phi^{[s]}\right)\alpha_{[s]}^{m+1,n+1},\\ &= \left(\mathcal{B}\Phi^{[s]}\right)\left(\Phi^{[s]}\right)^{-1}\varphi_{[s]}^{m+1,n+1} = \sigma^{[s]}\varphi_{[s]}^{m+1,n+1} = \sigma\varphi^{m+1,n+1},\end{aligned} \tag{25}$$

where $\sigma^{[s]} = \left(\mathcal{B}\Phi^{[s]}\right)\left(\Phi^{[s]}\right)^{-1}$, and σ is the expansion of $\sigma^{[s]}$ obtained by completing the local vector with zeros.

We substitute the Eqs. (24) and (25) into Eq. (18) to obtain the following system:

$$\begin{cases} \mathcal{L}^m \varphi^{m+1,n+1}(\boldsymbol{x}_s) = \Lambda^m(\boldsymbol{x}_s)\varphi^{m+1,n+1} = f^{m+1,n+1}(\boldsymbol{x}_s), \\ \mathcal{B}\varphi^{m+1,n+1}(\boldsymbol{x}_s) \quad = \sigma(\boldsymbol{x}_s)\varphi^{m+1,n+1} = q(\boldsymbol{x}_s), \end{cases} \tag{26}$$

which leads to the following sparse system:

$$\begin{pmatrix} \Lambda^m(\boldsymbol{x}_1) \\ \Lambda^m(\boldsymbol{x}_2) \\ . \\ . \\ . \\ \Lambda^m(\boldsymbol{x}_{n_i}) \\ \sigma(\boldsymbol{x}_{n_{i+1}}) \\ . \\ . \\ . \\ \sigma(\boldsymbol{x}_N) \end{pmatrix} = \begin{pmatrix} \varphi^{m+1,n+1}(\boldsymbol{x}_1) \\ \varphi^{m+1,n+1}(\boldsymbol{x}_2) \\ . \\ . \\ . \\ \varphi^{m+1,n+1}(\boldsymbol{x}_{n_i}) \\ \varphi^{m+1,n+1}(\boldsymbol{x}_{n_i+1}) \\ . \\ . \\ . \\ \varphi^{m+1,n+1}(\boldsymbol{x}_N) \end{pmatrix} \begin{pmatrix} f^{m+1,n+1}(\boldsymbol{x}_1) \\ f^{m+1,n+1}(\boldsymbol{x}_2) \\ . \\ . \\ . \\ f^{m+1,n+1}(\boldsymbol{x}_{n_i}) \\ q(\boldsymbol{x}_{n_i+1}) \\ . \\ . \\ . \\ q(\boldsymbol{x}_N) \end{pmatrix}. \tag{27}$$

The matrix generated by the localized RBF is sparse due to the presence of the local configuration in the solution approximation. This allows us to avoid ill-conditioned issues that arise in dense systems of equations generated by the global approach. By solving Eq. (27), we obtain the approximate values of $\varphi^{m+1,n+1}$ at all nodes $\varphi^{m+1,n+1}(\boldsymbol{x}_s)$, $s = 1, 2, ..., N$ of the computational domain.

4 Numerical Tests

In this section, we perform numerical experiments for solving the Richards equation by using the obtained Eq. (27) in one and two-dimensional systems. We used the localized RBF method based on the multiquadric radial basis function. For the temporal discretization, we used the backward Euler method.

4.1 One Dimensional Infiltration Problem

In this numerical test, we used the Brooks-Corey model [4] which describes the pressure head and the power law for the relative permeability.

$$J(S) = S^{-1/\lambda},\ k_r = S^{\beta} = \begin{cases} \left(\dfrac{h}{h_{cap}}\right)^{-\lambda\beta}, & \text{if } h \geq h_{cap}, \\ 1, & \text{if } h < h_{cap}. \end{cases} \tag{28}$$

Table 1 Hydraulic property parameters of 2 types of soil

Texture	θ_r	θ_s	θ_0	K_s	h_{cap}	λ	$\lambda\beta$
Sandy clay	0.109	0.321	0.121	0.002	29.15	0.168	2.504
Loam	0.027	0.463	0.040	0.022	11.15	0.220	2.660

where λ and β are respectively the parameters related to the Brook-Corey model and the power law for the relative permeability. The second (inequality) condition for the capillary pressure in Eq. (28) is introduced to avoid numerical issues [12, 14].

We consider two different types of soils with a depth L and their hydraulic parameters are shown in Table 1. We simulate a one-dimensional infiltration problem using the proposed method. In order to verify the effectiveness of the developed numerical model, we compare our numerical results with the numerical solutions of 1D-Hydrus where we consider the following initially and boundary conditions:

$$\begin{cases} \theta(z,0) = \theta_0, \\ \theta(0,t) = \theta_s, \\ \theta(L,t) = \theta_0, \end{cases} \tag{29}$$

Fig. 1 shows the numerical solutions obtained using the proposed method and 1D-Hydrus solutions where we observe good agreement between the solutions.

Table 2 presents the root mean squared error (RMSE), the relative error (L^1_{er}) between the numerical solutions and the solutions simulated by 1D-Hydrus. The results confirm the accuracy of the proposed method in modelling unsaturated flow in soils.

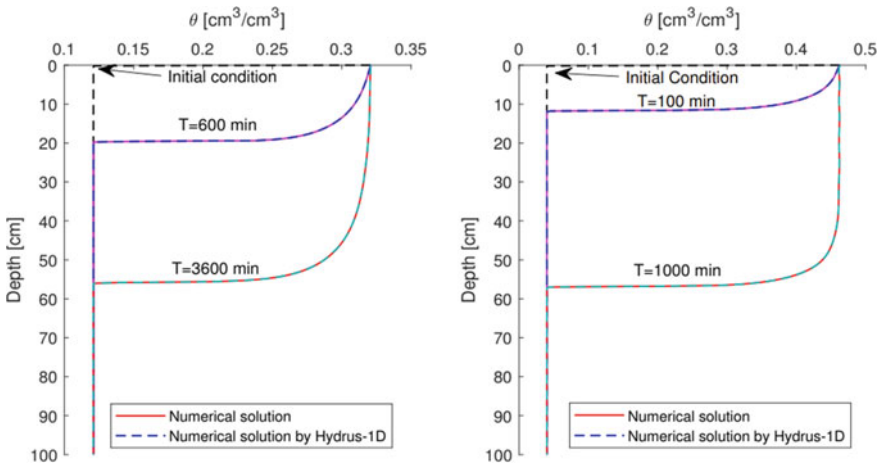

Fig. 1 Time evolution of moisture content for the soils given in Table 1. Left (Sandy clay), right (Loam)

Table 2 The RMSE and the L^1_{er} between the numerical solutions and 1D-Hydrus solutions

Soils	T(min)	RMSE	L^1_{er}
Sandy clay	600	5×10^{-3}	3.5×10^{-3}
	3500	5.8×10^{-3}	4.3×10^{-3}
Loam	100	4.8×10^{-3}	1.08×10^{-3}
	1000	6×10^{-3}	7.2×10^{-3}

4.2 Two-Dimensional Infiltration Problem

In this example, we perform numerical simulations using the proposed method for a two-dimensional infiltration problem where we consider a rectangular domain $[0, l] \times [0, L]$. We used the same hydraulic parameters of test 1 (Table 1) and $l = L = 100$ cm. We consider the following initial and boundary conditions:

$$\begin{cases} \theta(x, z, 0) = \theta_0, \\ \theta(x, 0, t) = \theta_s, \\ \theta(x, L, t) = \theta_0, \end{cases} \tag{30}$$

and no-flux boundary conditions are imposed on the sides $x = 0$ and $x = l$ of the domain.

The numerical simulations are performed using $N_x = 200$, $N_z = 200$, $\Delta t = 0.05$, and the localized RBF parameters $\varepsilon = 0.6$ and $n_s = 5$. The sandy clay and loam soils are selected in this numerical test to simulate unsaturated flow through a two-dimensional homogeneous medium. The time evolution of the total mass per unit of length of the 2D numerical solutions and the solutions simulated by 1D-Hydrus for a computational domain of unit length (1D problem) are displayed in Fig. 2. We observe good agreement between the solutions, which demonstrates the accuracy of

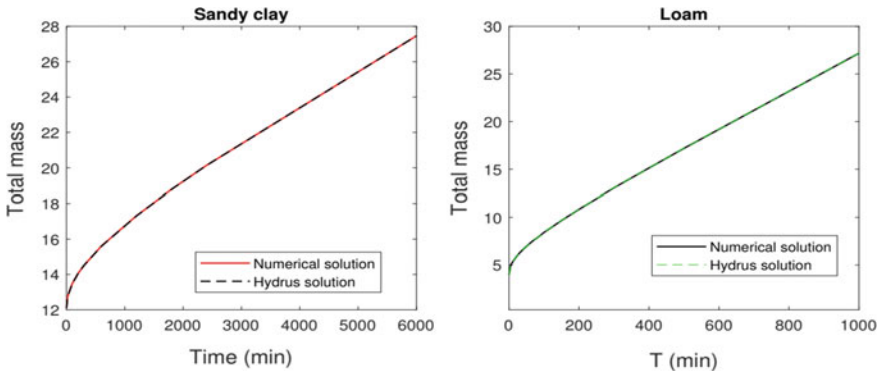

Fig. 2 Time-evolution of the total mass per unit of length of the sandy clay and loam soils

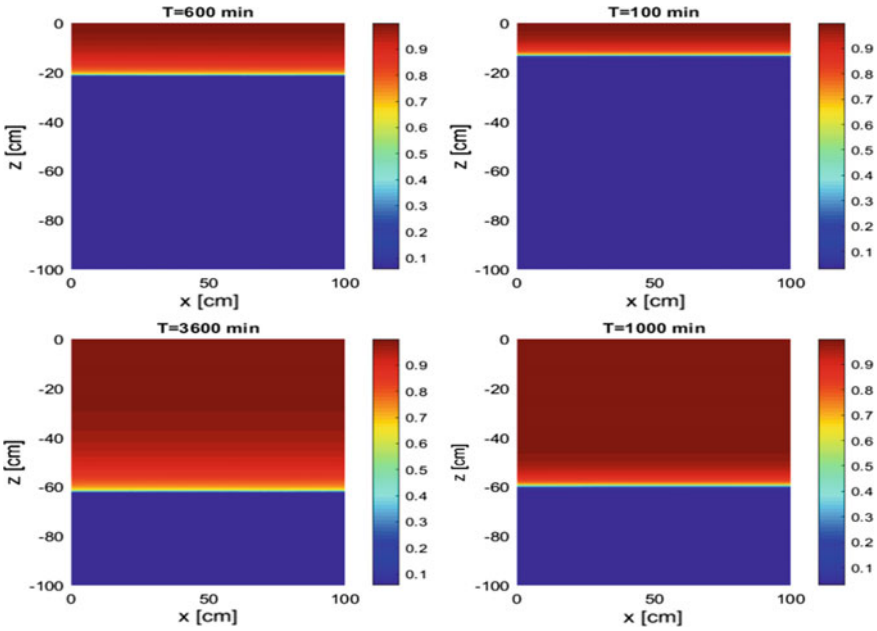

Fig. 3 The time evolution of saturation for the sandy clay (left) and loam (right) soils

the proposed method in modelling 2D unsaturated flow in soils. Figure 3 shows the time evolution of saturation for the sandy clay and loam considered soils.

The proposed method is efficient and accurate for solving the Richards equation. The method can be used for modelling unsaturated flow through homogeneous soils.

5 Conclusion

This paper focused on the infiltration process in porous media and introduced computational techniques for efficiently solving the Richards equation in one- and two-dimensional homogeneous medium. The proposed techniques using the Kirchhoff transformation allow us to reduce the nonlinearity of the obtained system from the Richards equation. Our approach using a localized radial basis function method avoiding mesh generation allows us to reduce the computational cost. The accuracy of the proposed method was validated using comparison between the numerical solutions and the results of 1D-Hydrus. Our results confirm the accuracy of the proposed techniques and their efficiency in terms of computational cost for solving the Richards equation. The numerical techniques proposed in this study for modelling unsaturated flow through homogeneous porous media is a first step toward developing efficient and accurate numerical methods for modelling unsaturated flows though heterogenous soils.

References

1. Bause M, Knabner P (2004) Computation of variably saturated subsurface flow by adaptive mixed hybrid finite element methods. Adv Water Resour 27:565–581
2. Bear J (1972) Dynamics of fluids in porous media. In: Courier Corporation. American Elsevier Publishing Company, New York
3. Boujoudar M, Beljadid A, Taik A (2021) Localized MQ-RBF meshless techniques for modeling unsaturated flow. Engineering Analysis With Boundary Elements 130:109–123
4. Brooks R, Corey T (1964) HYDRAU uc properties of porous media. Hydrology Papers, Colorado State University 24:37
5. Celia MA, Bouloutas ET, Zarba RL (1990) A general mass-conservative numerical solution for the unsaturated flow equation. Water Resour Res 26:1483–1496
6. Gardner WR (1958) Some steady-state solutions of the unsaturated moisture flow equation with application to evaporation from a water table. Soil Sci 85:228–232
7. Huang RQ, Wu LZ (2012) Analytical solutions to 1-D horizontal and vertical water infiltration in saturated/unsaturated soils considering time-varying rainfall. Comput Geotech 39:66–72
8. Ji SH, Park YJ, Sudicky EA, Sykes JF (2008) A generalized transformation approach for simulating steady-state variably-saturated subsurface flow. Adv Water Resour 31:313–323
9. Kansa EJ (1990) Multiquadrics—A scattered data approximation scheme with applications to computational fluid-dynamics—II solutions to parabolic, hyperbolic and elliptic partial differential equations. Comput Math Appl 19(1):147–161
10. Kansa EJ (1990) Multiquadrics—a scattered data approximation scheme with applications to computational fluid-dynamics—I surface approximations and partial derivative estimates. Comput Math Appl 19:127–145
11. Lee CK, Liu X, Fan SC (2003) Local multiquadric approximation for solving boundary value problems. Comput Mech 30:396–409
12. Lenhard RJ, Parker JC, Parker MS (1989) On the correspondence between Brooks-Corey and van Genuchten models. J Irrig Drainage Eng 115:744–751
13. Leverett M (1941) Capillary behavior in porous solids. Trans AIME 142:152–169
14. Ma Q, Hook JE, Ahuja LR (1999) Influence of three-parameter conversion methods between van Genuchten and Brooks-Corey functions on soil hydraulic properties and water-balance predictions. Water Resour Res 35:2571–2578
15. Manzini G, Ferraris S (1990) Mass-conservative finite volume methods on 2-D unstructured grids for the Richards' equation. Adv Water Resour 27:1483–1496
16. Richards LA (1931) Capillary conduction of liquids through porous mediums. Physics 1:318–333
17. Sander GC, Parlange JY, Kühnel V, Hogarth WL, Lockington D, O'kane JPJ (1988) Exact nonlinear solution for constant flux infiltration. J Hydrol 97:341–346
18. Srivastava R, Yeh TCJ(1991) Analytical solutions for one-dimensional, transient infiltration toward the water table in homogeneous and layered soils. Water Resour Res 27:753–762
19. Tracy FT (2011) Analytical and numerical solutions of Richards' equation with discussions on relative hydraulic conductivity. In: BoD—Books on demand
20. Van Genuchten MT (1980) A closed-form equation for predicting the hydraulic conductivity of unsaturated soils. Soil Sci Soc Am J 44:892–898